

EROSION STUDY OF TUNNEL 1 OF TARBELA DAM^{*}

M. ABID^{1**} A. A. NOON² AND H. A. WAJID³

^{1,2}Faculty of Mechanical Eng., Ghulam Ishaq Khan Institute of Eng. Sciences and Technology, Topi, Pakistan
Email: abid@giki.edu.pk

³Dept. of Mathematics, COMSATS Institute of Information Technology, Lahore, Pakistan

Abstract– In this paper, turbulent flow causing erosion in Tunnel 1 of Tarbela Dam using Reynolds Stress Model considering the effect of sediment particles is discussed. Velocity, pressure and erosion rate results are presented for three different water heads in the reservoir i.e., considering summer, winter and average seasons both for one-way and two-way/full coupling. Erosion rate is concluded the maximum at main bend and outlets at high head at full coupling. Numerical results are compared with the experimental erosion results for the scale down model of almost similar geometrical components. In addition, maximum loss of mass at T section in the loop with time is concluded.

Keywords– Tunnel erosion, turbulent flow, sediment particles, coupling

1. INTRODUCTION

Tarbela dam is one of the largest earth filled dams in the world. The increasing inflow of sediments in Tarbela reservoir is reducing its water storage capacity. Moreover, this increase of sediment particles is damaging the walls of tunnels, installed power generating units and is a severe threat to the main power generating hub in Pakistan. Tarbela dam is comprised of six tunnels, three of which are used for power generation and three for irrigation purposes. Tunnel 1 is used for power generation [1, 2]; its details are given in Table 1. In a related work, Hossain *et al* [3] have investigated the particle deposition and suspension in a horizontal pipe flow. The deposition was studied as a function of particle diameter, density and velocity of fluid. The lighter particles were found to remain suspended with homogeneous distribution. The larger particles clearly showed deposition near the bottom of the wall. In our work the diameter of the flow passage is very large; the results show the dependence of velocity, pressure and erosion rate density on the passage diameter. Xianghui *et al* [4] presented a computational fluid dynamics (CFD)-based erosion prediction model and its application to oilfield geometries, specifically elbows and plugged tee geometries. This comprehensive procedure consists of three major components: flow simulation, particle tracking, and erosion calculation. The analysis procedure is taken from this study but cavitation analysis procedure is different from this. Gary [5] explains the Lagrangian approach for particle tracking, authors have used the same approach in one way coupling but Eulerian approach is used for two way coupling. Hari [6] explains the role of different forces when a solid particle passes through a fluid, but in our case the rotational force is ignored.

One-way and two-way/full coupling options are used depending upon the value of β , which is defined as the ratio of the particulate mass per unit volume flow to the fluid mass per unit volume flow and is taken as 0.2 as a threshold value [5]. One-way coupling is valid for volume concentration up to 14.86%

*Received by the editors July 11, 2013; Accepted January 22, 2014.

**Corresponding author

and simply predicts particle paths during post-processing based on the flow field without affecting the flow field (i.e. particles are assumed not to interact with each other). In two way/full coupling particles exchange momentum with continuous phase, allowing the continuous flow to affect the particles and vice versa.

Table 1. Details of tunnel 1 [2]

Parameter	Value
Length (m)	786.4
Inlet elevation (m)	373.4
Elevation of straight portion (m)	339.16
Inlet diameter (m)	10.96
Outlet branch diameter (m)	4.87
Outlet elevation (m)	337.11
High head (kPa)	1307.039
Medium head (kPa)	934.025
Low head (kPa)	561.0122
Average volume flow rate (m ³ /s)	656.016
Material of the steel liner	High strength low alloy steel (A-441)
Steel liner thickness (cm)	5.4-6.35
Quantity of turbines for power generatio (Nos)	4
Capacity of each turbine (MW)	175
For four turbines (MW)	700

For analysis of turbulent flow in Tunnel 1, we use second-moment closure model or Reynolds stress model (RSM) [3] and different coefficients used are taken from [7-11]. For sediment particles deposition in turbulent flow, Lagrangian particle transport and Eulerian-Eulerian multiphase approaches are used [12] in conjunction with RANS framework. Moreover, to determine the erosion rate under turbulent flow in the tunnel for different heads, ANSYS CFX [13] is used.

Generally, a small, rigid spherical particle entrained in the turbulent pipe flow encounters many forces [6]. In general, n varies between 2 and 3 depending on both the surface and particle materials. For the present study we have ignored the force of gravity on the particle, it is important to note that for most cases the gravitational acceleration is taken zero. One can include the gravity force, but should define the magnitude and direction of the gravity vector. Virtual mass force which is used to accelerate the fluid surrounding the particle is also ignored along with additional forces arising from the pressure gradient in the fluid and rotation of the reference frame. Later forces are important only when fluid is flowing in a rotating frame. Another force which is not relevant to our model is produced because of temperature gradient effecting small particles suspended in a gas. This phenomenon is known as thermophoresis. For micro particles, the effects of Brownian motion is optional and if required can be included in the additional force term. For one-way and two-way coupling, particle transport drag coefficient of 0.1 and 0.44 respectively are used [7-11].

Sediment erosion phenomenon is highly complicated and a wide range of factors contribute to erosion severity [14]. Analysis is done using Finnie with Lagrangian particle tracking and Eulerian-Eulerian multiphase approach.

Cutting wear occurs due to particle impacts at small angles, with a scratch or cut being formed on the surface if the shear strength of the material is exceeded. The other critical factor affecting wear is the particle impact velocity, with both cutting and deformation wear being proportional to impact velocity raised to a power n determined through physical tests. In general n varies between 2 and 3 depending on both the surface and particle materials.

2. MODELING AND ANALYSIS

Modeling of Tunnel 1 is done in Pro-Engineer software as shown in Fig. 1 [15]. Models are meshed in ICEM CFX with free mesh option using 1843803 tetrahedral elements Adaptive meshing uses 53210 elements at the critical locations (main bend, main branch and outlet branches). Meshed model is imported into ANSYS CFX [13] for detailed analysis [16] as shown in Fig. 2. A zero pressure is specified at the tunnel’s outlets being exposed to the atmosphere. The particles were assumed to be randomly distributed at the inlet. The particles injected at the inlet are proportional to the mass flow rate of the water flowing into the tunnel. The sediment particles volume fraction is only 0.007% at the high head during the months of July, August and September, which increases to 6.1% at the minimum head level in the months of March, April, May and June as per data collected in May 2008 [2]. Both the fractions fall in the one-way coupling phenomena. Standard no-slip wall functions were applied at all solid surfaces for the fluid phase and the coefficient of restitution for the particles was taken as 0.9 for the parallel coefficient and 1.0 for the perpendicular coefficient. During analysis, air relief valves are excluded in the geometry, which might affect the water velocities and pressures at different locations of the tunnels. Boundary and initial Conditions applied are summarized in Table 2 and list of other input parameters is given in Table 3.

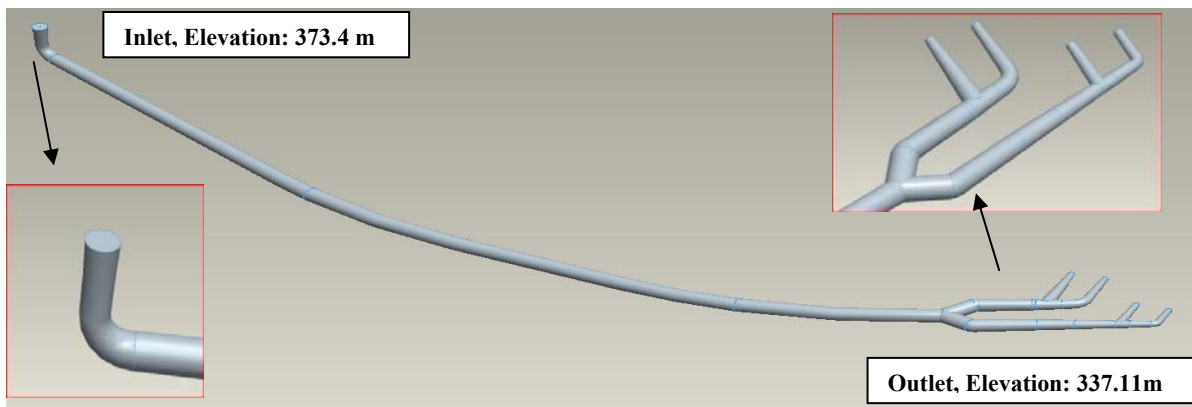


Fig. 1. Tunnel model

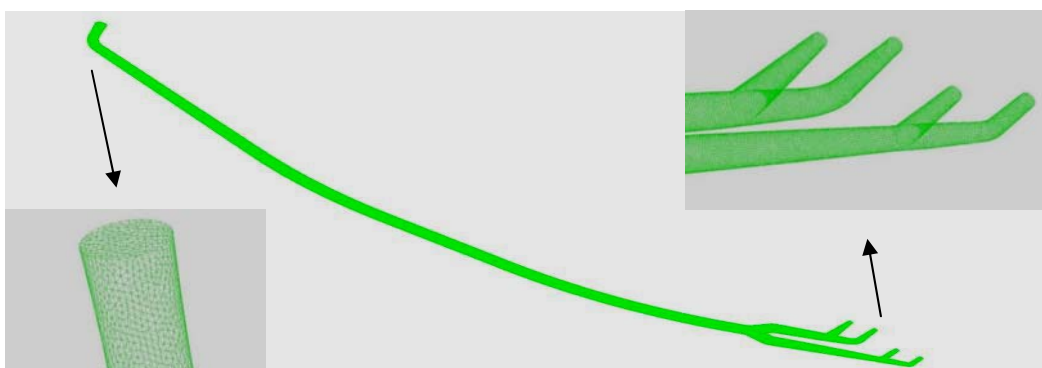


Fig. 2. Tunnel mesh

Table 2. Boundary conditions and Initial conditions

Type		Head	Value
BCs	Pressure (P) kPa	Low	561.01
		Medium	934.03
		High	1307.04
ICs	Velocity (V) ms ⁻¹	Low	5.24
		Medium	6.94
		High	8.44

Table 3. Input parameters used in Numerical Analysis using ANSYS CFX

Sr #	Parameter	Details	Coefficients/values
1	Mass flow rate	Sediment particles mass flow rate at high head	$23.17e^{-5}$ kg/s
2	Erosion model	Finnie	$k = 1.0$ and $n = 2.0$
3	Particles injection	Uniform injection at the tunnel inlet	6.1% particles for one-way coupling and more than 15% particles for full coupling
4	Wall roughness	At the wall	0.2 mm
5	Restitution coefficients	Parallel and perpendicular based on impact and rebound velocities	0.9 and 1.0
6	Drag force	Schiller and Naumann correlation for the evaluation of drag coefficient	0.44
7	Numerical Scheme	Specified blend factor	1.0
8	Particle integration	Tracking distance and time	786.4 m and 300 s

3. RESULTS AND DISCUSSION

Maximum velocities of the sediment particles 61.94, 83.48 and 94.53 m/s are observed at low, medium and high head of water respectively at the inner periphery of the main bend. After the main bend, the velocity decreases to 31.02, 41.68 and 47.41 m/s respectively at low, medium and high water heads. Velocity finally reduces to 15.56, 21.08 and 23.85 m/s when the water flow is fully developed at 150 m from the vertical section at low, medium and high water head respectively. The velocity increases abruptly at the outlet branches due to the reduction in the area at these locations.

Maximum pressures of the sediment particles 847.30, 1385 and 1975 kPa are observed at the fully developed flow location, i.e 150 m from the vertical section at low, medium and high water heads respectively. The minimum pressures 33, 136.75 and 140 kPa are observed at the inner periphery of the main bend where the velocity has its highest value respectively at low, medium and high water heads. The pressure decreases abruptly at the main branch and at the outlet branches due to the increase in the velocity at these locations.

The maximum erosion rate density of the sediment particles 2.11×10^{-5} , 4.03×10^{-5} , 5.97×10^{-5} $\text{kgs}^{-1}\text{m}^{-2}$ for one way coupling and 1.08×10^{-5} , 2.07×10^{-5} , 4.77×10^{-5} $\text{kgs}^{-1}\text{m}^{-2}$ for two way/full coupling are observed at low, medium and high head of water respectively at the inner periphery of the main bend. It changes abruptly at the main branch and at the outlet branches due to the higher impact velocity and impact angle at these locations.

The velocity, pressure and erosion density rate profiles at critical locations for two way/full coupling at the high head are shown in Figs. 3a-i. The velocity and pressure are the maximum at high head in the months of July, August and September which are the most critical period for erosion damage [Table 4]. The medium head remains for five months, i.e. April, May, June, October and November, when the velocity and pressure are measured moderate. The low head remains for four months, i.e. December, January, February and March when the water velocity and pressure are measured to be the minimum.

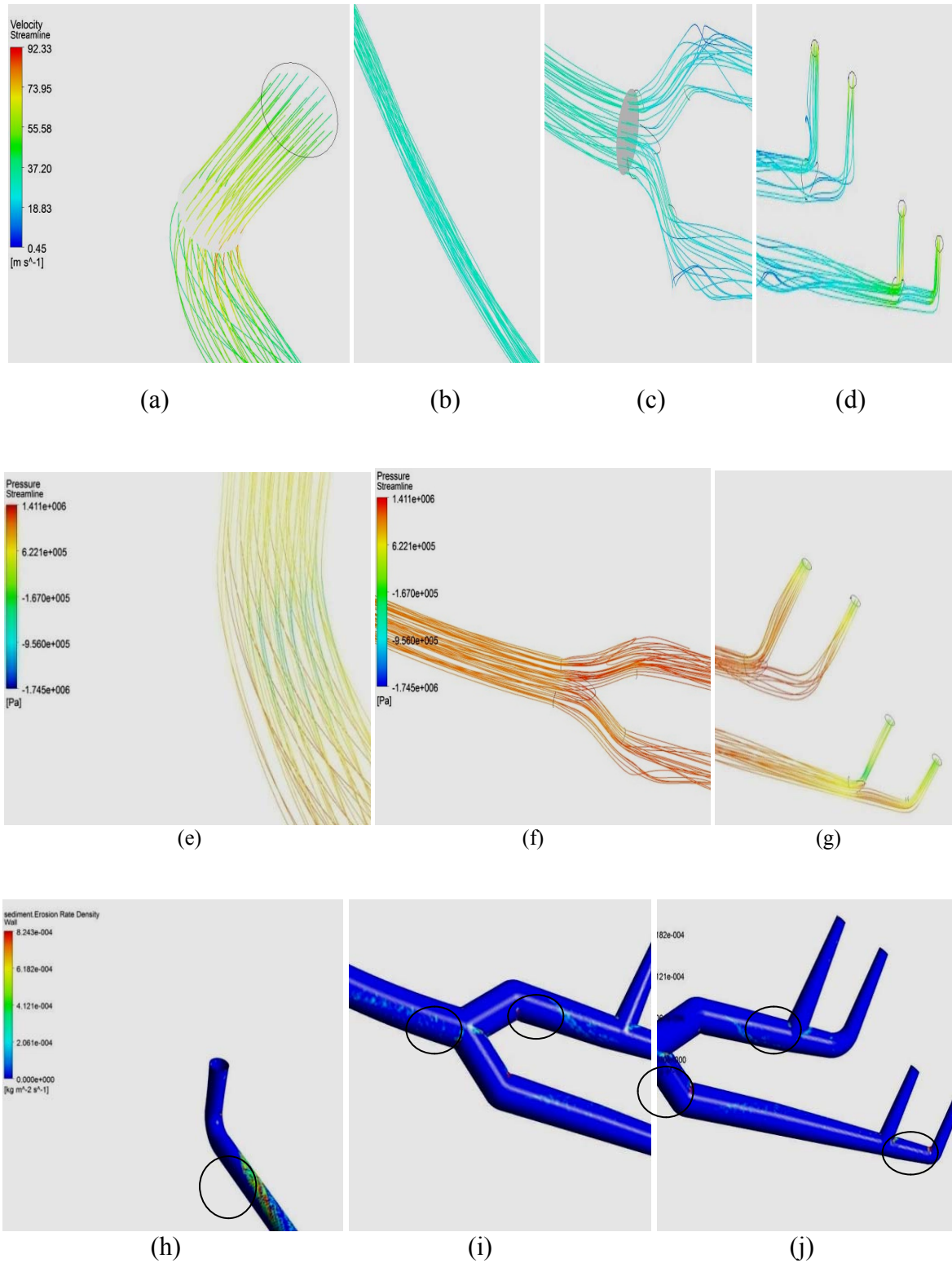


Fig. 3. Two way/full coupling with sediments at high head for: (a-d) velocity profiles, (e-g) pressure profiles and (h-j) erosion rate density profiles along, main bend, main branch, and outlet branches respectively

Table 4. Velocity, Pressure and Erosion rate density for tunnel at high head

Results	Criteria	Location						
		Main Bend	After Bend	Main Branch	Branch 1	Branch 2	Branch 3	Branch 4
Velocity (V) ms ⁻¹	One way coupling							
	Without sediments	95.23	47.91	24.43	65.33	65.33	65.33	65.33
	With sediments	94.53	47.41	23.85	64.93	64.93	64.93	64.93
	Full coupling							
	Low sediments conc.	83.48	41.68	21.08	49.43	49.43	49.43	49.43
Higher sediments conc.	98.77	51.63	26.93	68.31	68.31	68.31	68.31	
Pressure (P) kPa	One way coupling							
	Without sediments	34	1425.33	1978	319.56	319.56	319.56	319.56
	With sediments	33	1422.50	1975	318.70	318.70	318.70	318.70
	Full coupling							
	Low sediments conc.	27	936	1385	38.7	38.7	38.7	38.7
Higher sediments conc.	43	1234	1863	70.32	70.32	70.32	70.32	
Erosion rate density (E) 10 ⁻⁵ kgs ⁻¹ m ⁻²	One way coupling							
	Without sediments	-----	-----	-----	-----	-----	-----	-----
	With sediments	5.97	4.77	5.37	5.08	5.08	5.08	5.08
	Full coupling							
	Low sediments conc.	4.77	3.94	4.39	4.13	4.13	4.13	4.13
	Higher sediments conc.	6.86	5.97	6.33	5.91	5.91	5.91	5.91
	Impact velocity (V) ms ⁻¹ with sediments	94.53	47.41	23.85	64.93	64.93	64.93	64.93
Impact angle, γ with sediments	18.5° < γ < 90°	γ < 18.5°	18.5° < γ < 90°	γ < 18.5°	γ < 18.5°	18.5° < γ < 90°	18.5° < γ < 90°	

4. EXPERIMENTAL AND NUMERICAL ANALYSIS OF FLOW THROUGH SIMILAR GEOMETRIC COMPONENTS

An experimental setup is developed to validate the numerical results discussed in Section 5.2. The experimental setup is shown in Fig. 4a-d. The pipe loop is constructed in the horizontal plane with a valve to allow flow to be diverted to another loop as necessary. A high power stirrer is installed to help

distribute the sediments in the tank. Pipe components are made of AISI 304L stainless steel with a nominal wall thickness of 3 mm. The geometric components like straight portion, bend-section and T-section are all analyzed for their flow characteristics in this study. Pipe sections are prepared for weighing by firstly thoroughly rinsing with water to remove any sediment and then cleaned with warm 5% citric acid to remove calcite deposits on internal surfaces. This was necessary to allow the change in mass of the pipe sections to be attributed solely to erosion. The pipes are then allowed to air dry, usually overnight, prior to weighing. The experiment is performed for continuous flow of sediments for 80 hours with sediments concentration of about 0.4% by volume and a velocity of 0.175 m/s. The Reynolds number calculated is 2997 for this flow. The loops are then carefully dismantled for cleaning and weighing.

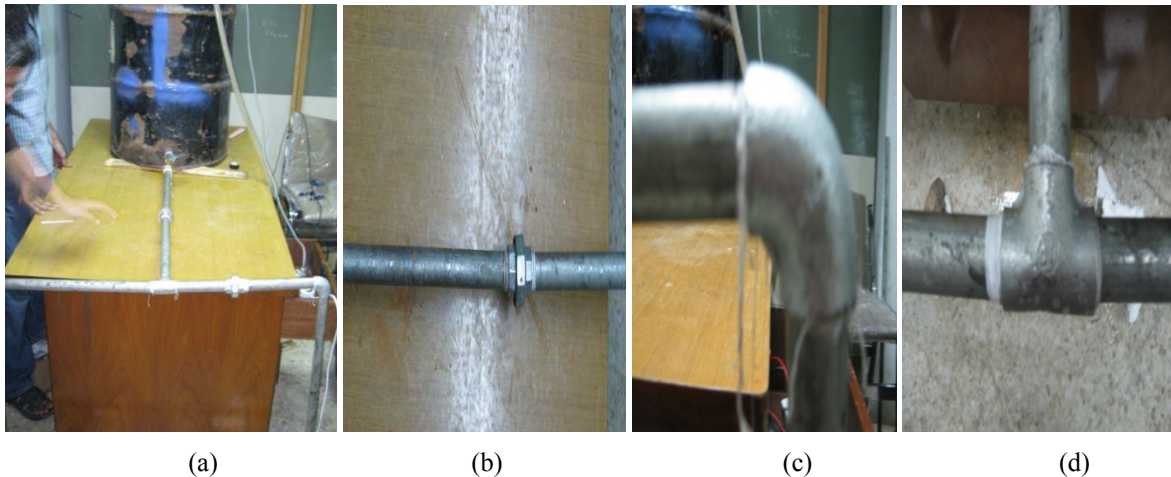


Fig. 4. (a) Complete experimental setup, (b) Straight portion, (c) Bend section, (d) T-section

Pro-Engineer Wildfire 4.0 is used for the modeling of the components, i.e. straight portion, bend-section and T-section. The ANSYS ICEM package is used for the meshing of the geometry. The number of elements used in the geometric components are 1500, 130 and 160 respectively. The analysis done in ANSYS CFX is shown in Fig. 5a-c. Comparative results between experimental and numerical results are given in Table 5. The results show an error of about 8% for erosion rate density. The circularity metric and aspect ratio calculated through particulate analysis show that the size of the sediment particles is reduced after they strike the tunnel walls. 11.54% reduction is observed in particle diameter after 20 hours of elapsed time for a particle concentration of (3-18)%, flowing with a velocity of (0.2-2) m/s. The removal of the material increases slowly in the beginning of the experiment but impedes as time progresses. Loss of mass at different sections of loop with time is plotted in Fig. 6.

Table 5. Comparison between Experimental and Numerical results

	Straight Portion	Bend Section	T-Section	
			Inlet	Outlets
Surface area (m ²)	2.736x10 ⁻²	5.428x10 ⁻³	5.963x10 ⁻³	
Volumetric flow rate (m ³ /s)	5.00x10 ⁻⁵	5.0010 ⁻⁵	1.00 10 ⁻⁴	5.00x10 ⁻⁵
Velocity (m/s)	0.175	0.175	0.350	0.175
Mass flow rate of water (m ³ /s)	0.0499	0.0499	0.0998	0.0499
Mass flow rate of sediments (m ³ /s)	1.923x10 ⁻⁴	1.923x 10 ⁻⁴	3.8454 10 ⁻⁴	1.92310 ⁻⁴
Change in mass (g)	4.98	7.45	11.01	
Erosion rate (kg/m ² .s)	6.319x10 ⁻⁷	4.766x10 ⁻⁶	6.411x10 ⁻⁶	
Erosion rate from CFX (kg/m ² .s)	6.909x10 ⁻⁷	4.960x10 ⁻⁶	6.638x10 ⁻⁶	
% difference	8.50	3.90	3.40	

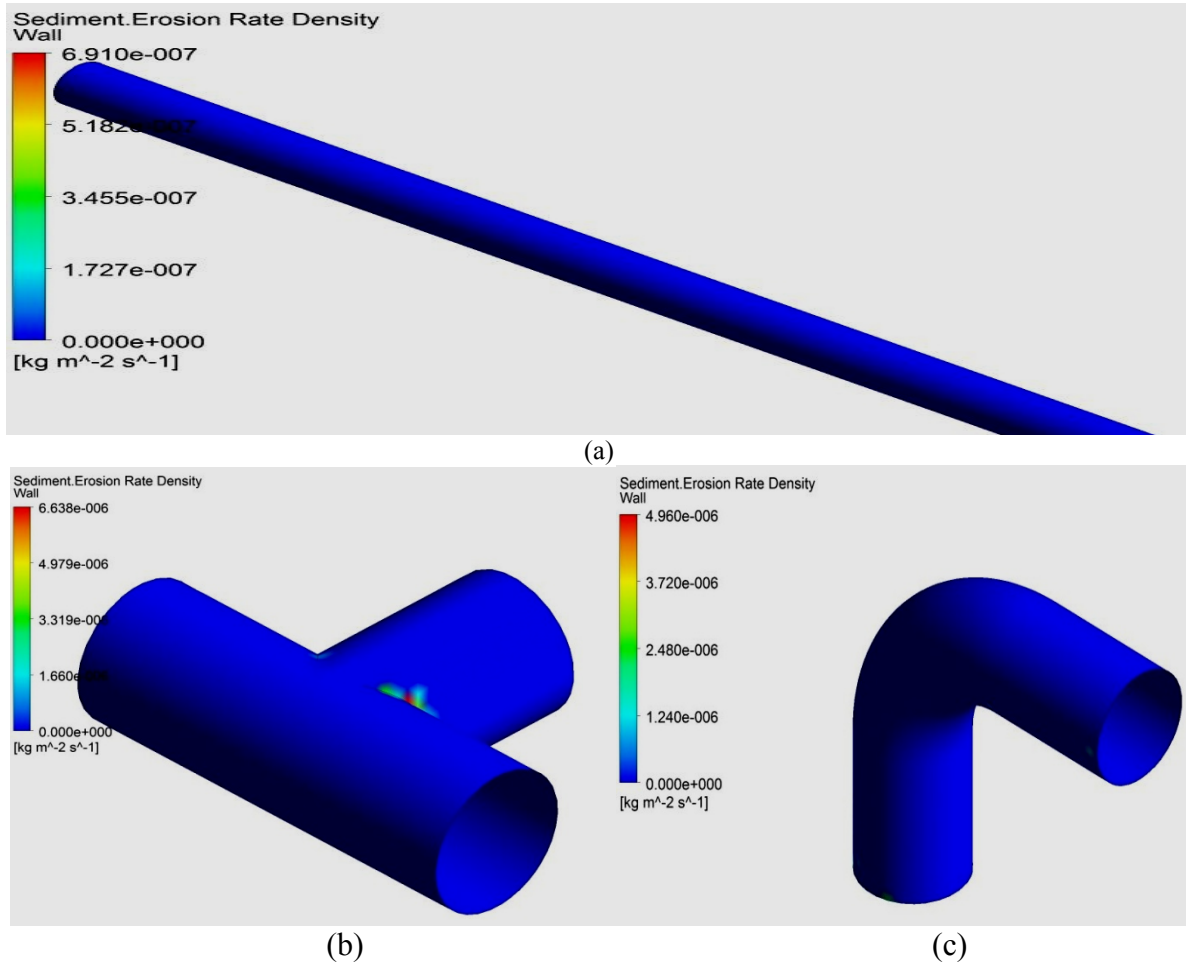


Fig. 5. Erosion rate density profiles for the: (a) Straight portion, (b) T-section, (c) Bend-section

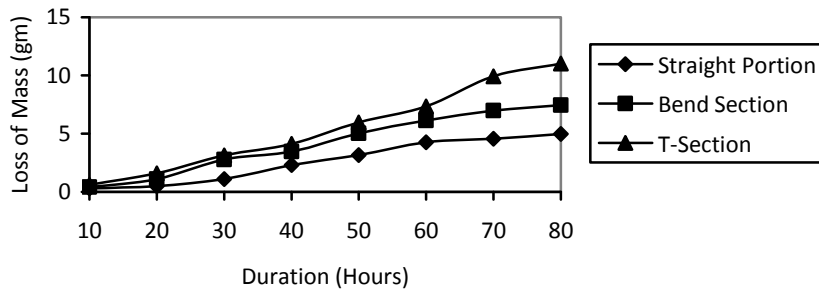


Fig. 6. Loss of mass with time in the components in the loop

5. CONCLUSION

High head is concluded critical because of the higher impact velocity and erosion rate during July, August and September. Erosion rate density is the maximum at the main bend and outlet branches due to several reasons like the higher impact velocity, impact angle and the production of turbulent eddies. No cavitation erosion was found at any location in the tunnel. Comparative numerical and experimental results show that a CFD-based erosion prediction procedure is able to reasonably predict the erosion profile and satisfactorily capture the trend of erosion with respect to the carrier velocity with an error of about 8.5% for the straight portion, 3.9% for the bend portion and 3.5% for the T-section. Maximum loss of mass with time is observed at the T section in the loop. Degradation of sediment particles is observed due to the

collisions with pipe walls. This increase in particle concentration is changing continuous flow (one way coupling) to dispersed flow (two way/full coupling) and damage to the tunnel is observed to be increasing.

REFERENCES

1. Cunkui, H., Chioveli, S., Minev, P., Jingli, L. & Nandakumar, K. (2008). A comprehensive phenomenological model for erosion of materials in jet flow. *Powder Technology*, Vol. 187, No. 3, pp. 273-279.
2. Hanif, M. (2009). Sediment concentration (ppm). *Annual Reservoir Sedimentation Report, Survey and Hydrology Department, Tarbela Dam Project*, p. 5.
3. Hossain, A., Naser, J., Macmanus, K. & Ryan, G. (2006). CFD Investigation of Particle Deposition and Distribution in a Horizontal Pipe. *3rd Intl. Conf. on CFD in the Process Industries. Melbourne, Australia*. 10-12, December 2006, pp. 489-492.
4. Xianghui, C., Brenton, S. M. & Siamack A. S. (2004). Application and experimental validation of a computational fluid dynamics (CFD) based erosion prediction model in elbows and plugged tees. *Computers & Fluids*. Vol. 33, pp. 1251-1272.
5. Gary, B. (2006). Use of CFD to predict and reduce erosion in industrial slurry piping system. *5th Intl Conf. on CFD in the Process Industries. CSIRO, Melbourne, Australia*. 13-15 December, 2006, pp. 1-10.
6. Hari, P. N. (2010). Faculty of engineering science and technology, norwegian university of science and technology (NTNU). *PhD Thesis*. Trondheim, Norway.
7. Abid, M., Noon, A. A. & Wajid, H. A. (2010). Simulations of turbulent flow through Tarbela Dam Tunnel 3. *IJUM Engineering Journal*. Vol. 11, No. 2, pp. 201-224.
8. Abid, M., Noon, A. A. & Wajid, H. A. (2010). Turbulent flow simulations through Tarbela dam tunnels considering the effect of sediment particles. *10th Biennial ASME Conference on Engineering Systems Design and Analysis (ESDA)*. Istanbul, 12-14 July 2010, pp. 1-6.
9. Abid, M. & Noon, A. A. (2010). Turbulent flow simulations through Tarbela dam tunnel-2. *Journal of Engineering*. Vol. 2, No. 7, pp. 205-213.
10. Abid, M. & Noon, A. A. (2010). Study of the effect of sediment flows through Tarbela Dam tunnels. *ISFCS2010 Islamabad Pakistan*, pp. 1-16.
11. Abid, M., Noon, A. A. & Rehman, M. (2011). Water and sediment flow simulations for Tarbela reservoir and tunnels. *VDM Verlag Dr.Muller*, ISBN: 978-3-639-34183-6.
12. Dosanjh, S. & Humphrey, J.A.C. (1985). The influence of turbulence on erosion by a particle laden fluid jet. Vol. 102, pp. 309-330.
13. ANSYS CFX. (2006). *Reference Guide. Release 11*. pp. 1-4.
14. Bouhadji, L. (2003). Three dimensional numerical simulation of turbulent flow over spillways. *ASL-AQFlow Inc., Sidney, British Columbia, Canada*, pp 1-7.
15. Pro/Engineer. (2009). *Wildfire Release 4*.
16. Tippets & Abbett. (1967). Civil engineering works. *Contract Documents for Construction of Tarbela Dam Project. TAMS, International*. Vol. 6, pp. 16.